J|A|C|S
ARTICLES
Published on Web 01/04/2007

Dimerization of Alkynes Promoted by a Pincer-Ligated Iridium Complex. C−C Reductive Elimination Inhibited by Steric Crowding

Rajshekhar Ghosh, Xiawei Zhang, Patrick Achord, Thomas J. Emge, Karsten Krogh-Jespersen,* and Alan S. Goldman*

Contribution from the Department of Chemistry and Chemical Biology, Rutgers, the State University of New Jersey, Piscataway, New Jersey 08854

Received July 16, 2006; E-mail: alan.goldman@rutgers.edu; krogh@rutchem.rutgers.edu

Abstract: The pincer-ligated species (PCP)Ir (PCP = κ^3-C_6H_3-2,6-$(CH_2P^tBu_2)_2$) is found to promote dimerization of phenylacetylene to give the enyne complex (PCP)Ir(*trans*-1,4-phenyl-but-3-ene-1-yne). The mechanism of this reaction is found to proceed through three steps: (i) addition of the alkynyl C−H bond to iridium, (ii) insertion of a second phenylacetylene molecule into the resulting Ir−H bond, and (iii) vinyl−acetylide reductive elimination. Each of these steps has been investigated, by both experimental and computational (DFT) methods, to yield unexpected conclusions of general interest. (i) The product of alkynyl C−H addition, (PCP)Ir(CCPh)(H) (**3**), has been isolated and, in accord with experimental observations, is calculated to be 29 kcal/mol more stable than the analogous product of benzene C−H addition. (ii) Insertion of a second PhCCH molecule into the Ir−H bond of **3** proceeds rapidly, but with a 1,2-orientation. This orientation gives (PCP)Ir(CCPh)(CPh=CH_2) (**4**) which would yield the 1,3-diphenyl-enyne if it were to undergo C−C elimination; however, the insertion is reversible, which represents the first example, to our knowledge, of simple β-H elimination from a vinyl group to give a terminal hydride. The 2,1-insertion product (PCP)Ir(CCPh)(CH=CHPh) (**6**) forms more slowly, but unlike the 1,2 insertion product it undergoes C−C elimination to give the observed enyne. (iii) The failure of **4** to undergo C−C elimination is found to be general for (PCP)Ir(CCPh)(vinyl) complexes in which the vinyl group has an α-substituent. Thus, although C−C elimination *relieves* crowding, the reaction is *inhibited* by increased crowding. Density-functional theory (DFT) calculations support this surprising conclusion and offer a clear explanation. Alkynyl−vinyl bond formation in the C−C elimination transition state involves the vinyl group π-system; this requires that the vinyl group must rotate (around the Ir−C bond) by ca. 90° to achieve an appropriate orientation. This rotation is severely inhibited by steric crowding, particularly when the vinyl group bears an α-substituent.

Introduction

The formation of carbon−carbon bonds is the foundation of organic chemical synthesis. Regioselective activation of a C−H bond, followed by carbon−carbon bond formation, is accordingly an extremely attractive challenge that has become the subject of intense study in recent years.[1] Particularly since the report by Murai of ruthenium-catalyzed regioselective addition of aryl C−H bonds across C−C double bonds,[2] considerable advances have been made by several groups[3−6] in the use of transition-metal complexes to promote such reactions. Perhaps the most conceptually straightforward pathways for such transformations generally involve C−H addition by a metal center, followed by insertion of an unsaturated species into either a metal−carbon or metal−hydrogen bond, and then elimination of either C−H or C−C bonds, respectively (see Scheme 1).

The Murai systems, for example, have been shown to proceed via the latter type of pathway, that is, olefin insertion into a Ru−H bond followed by C−C elimination.[2]

One example of catalytic addition of a C−H bond across a multiple bond, that has been fairly well developed, is the dimerization of acetylenes, eq 1.[7−38]

(1) (a) Guari, Y.; Sabo-Etiennne, S.; Chaudret, B. *Eur. J. Inorg. Chem.* **1999**, 1047−1055. (b) Ritleng, V.; Sirlin, C.; Pfeffer, M. *Chem. Rev.* **2002**, *102*, 1731−1769. (c) Jun, C.-H.; Lee, J. H. *Pure Appl. Chem.* **2004**, *76*, 577−587.
(2) (a) Murai, S.; Kakiuchi, F.; Sekine, S.; Tanaka, Y.; Kamatani, A.; Sonoda, M.; Chatani, N. *Nature* **1993**, *366*, 529−531. (b) Kakiuchi, F.; Murai, S. *Acc. Chem. Res.* **2002**, *35*, 826−834.
(3) Weissman, H.; Song, X.; Milstein, D. *J. Am. Chem. Soc.* **2001**, *123*, 337−338.
(4) (a) Matsumoto, T.; Taube, D. J.; Periana, R. A.; Taube, H.; Yoshida, H. *J. Am. Chem. Soc.* **2000**, *122*, 7414−7415. (b) Matsumoto, T.; Periana, R. A.; Taube, D. J.; Yoshida, H. *J. Mol. Catal. A: Chem.* **2002**, *180*, 1−18. (c) Periana, R. A.; Liu, X. Y.; Bhalla, G. *Chem. Commun.* **2002**, 3000−3001. (d) Bhalla, G.; Oxgaard, J.; Goddard, W. A., II; Periana, R. A. *Organometallics* **2005**, *24*, 5499−5502. (e) Bhalla, G.; Oxgaard, J.; Goddard, W. A., III; Periana, R. A. *Organometallics* **2005**, *24*, 3229−3232. (f) Oxgaard, J.; Bhalla, G.; Periana, R. A.; Goddard, W. A., III. *Organometallics* **2006**, *25*, 1618−1625.
(5) (a) Lail, M.; Arrowood, B. N.; Gunnoe, T. B. *J. Am. Chem. Soc.* **2003**, *125*, 7506−7507. (b) Goj, L. A.; Gunnoe, T. B. *Curr. Org. Chem.* **2005**, *9*, 671−685.
(6) (a) Thalji, R. K.; Ellman, J. A.; Bergman, R. G. *J. Am. Chem. Soc.* **2004**, *126*, 7192−7193. (b) Thalji, R. K.; Ahrendt, K. A.; Bergman, R. G.; Ellman, J. A. *J. Am. Chem. Soc.* **2001**, *123*, 9692−9693.
(7) Hoehn, A.; Werner, H. *J. Organomet. Chem.* **1990**, *382*, 255−272.
(8) Werner, H.; Brekau, U. *Z. Naturforsch., B: Chem Sci.* **1989**, *44*, 1438−1446.

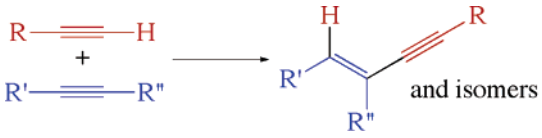

(1)

Although this may be considered a somewhat "easy" case, since the acetylenic C−H bond is generally much more reactive than sp^3 or even sp^2 C−H bonds (and C−C triple bonds are generally more reactive than double bonds[39]), we felt that a mechanistic study of acetylene dimerization could yield insights relevant to the broader class of C−H addition across multiple bonds. Herein we report the results of such a study, which has revealed unanticipated fundamental aspects of the insertion of alkyne bonds into M−H bonds, and, in particular, C−C bond elimination.

Results and Discussion

1. Phenylacetylene Dimerization. The reaction of (PCP)-IrH_2 (PCP = κ^3-C_6H_3-2,6-$(CH_2PR_2)_2$; R = ^{t}Bu for all experimental work, and for computational work as well unless noted otherwise) with 2 equiv norbornene (NBE) yields norbornane and a compound of the composition (PCP)Ir(NBE). Although not well characterized, "(PCP)Ir(NBE)" readily acts as a source of (PCP)Ir. Addition of 2 equiv phenylacetylene (PhCCH) to a xylene solution of this precursor results, after ca. 8 h at room temperature, in the clean formation of a single complex (**1**) as indicated by ^{31}P NMR. The ^{1}H NMR spectrum is consistent with characterization of **1** as an adduct of (PCP)Ir and the PhCCH dimerization product, *trans*-1,4-phenyl-but-3-ene-1-yne (**2**), as indicated in eq 2.

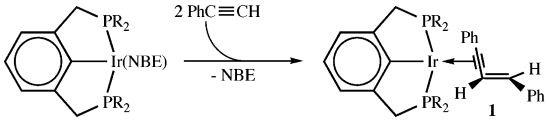

(2)

Support for this characterization was obtained by the addition of CO to the resulting solution, yielding (PCP)Ir(CO)[40] and **2** (eq 3). Enyne **2** was characterized (^{1}H and ^{13}C NMR) by comparison with a known sample[16] and by single-crystal X-ray diffraction of cocrystallized (PCP)Ir(CO) and **2** (Supporting Information).

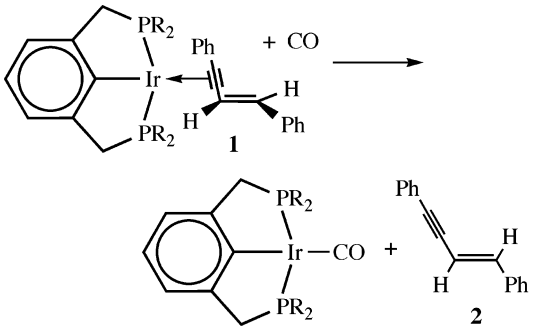

(3)

Crystals of **1** were obtained by slow evaporation of a pentane solution; the characterization of **1** as the (PCP)Ir adduct of **2** was confirmed by X-ray diffraction (Figure 1). The triple bond of the enyne is π-bound to the iridium center; the C−C triple bond distance is 1.270(4) Å, significantly greater than the crystal-

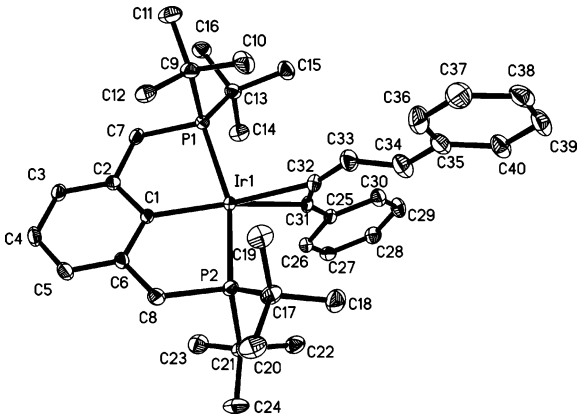

Figure 1. X-ray structure of (PCP)Ir(*trans*-1,4-phenyl-but-3-ene-1-yne) (**1**).

Scheme 1

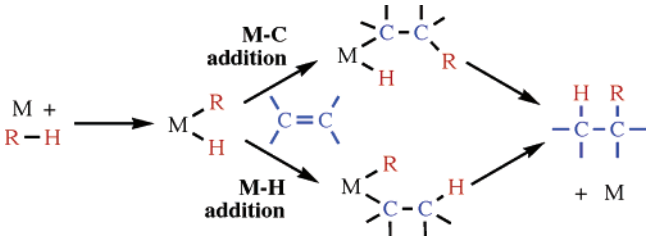

(9) Schaefer, M.; Mahr, N.; Wolf, J.; Werner, H. *Angew. Chem.* **1993**, *105*, 1377−1379.
(10) Schaefer, M.; Wolf, J.; Werner, H. *Organometallics* **2004**, *23*, 5713−5728.
(11) Werner, H. *Coord. Chem. Rev.* **2004**, *248*, 1693−1702.
(12) Krueger, P.; Werner, H. *Eur. J. Inorg. Chem.* **2004**, 481−491.
(13) Schaefer, M.; Wolf, J.; Werner, H. *J. Chem. Soc., Dalton Trans.* **2005**, 1468−1481.
(14) Weng, W.; Guo, C.; Celenligil-Cetin, R.; Foxman, B. M.; Ozerov, O. V. *Chem. Commun.* **2006**, 197−199.
(15) Ogoshi, S.; Ueta, M.; Oka, M.-A.; Kurosawa, H. *Chem. Commun.* **2004**, 2732−2733.
(16) Lee, C.-C.; Lin, Y.-C.; Liu, Y.-H.; Wang, Y. *Organometallics* **2005**, *24*, 136−143.
(17) Nishiura, M.; Hou, Z. *J. Mol. Catal. A: Chem.* **2004**, *213*, 101−106.
(18) Yang, C.; Nolan, S. P. *J. Org. Chem.* **2002**, *67*, 591−593.
(19) Boese, W. T.; Goldman, A. S. *Organometallics* **1991**, *10*, 782−786.
(20) Li, X.; Vogel, T.; Incarvito, C. D.; Crabtree, R. H. *Organometallics* **2005**, *24*, 62−76.
(21) Esteruelas, M. A.; Herrero, J.; Lopez, A. M.; Olivan, M. *Organometallics* **2001**, *20*, 3202−3205.
(22) Dash, A. K.; Eisen, M. S. *Org. Lett.* **2000**, *2*, 737−740.
(23) Trost, B. M.; Sorum, M. T.; Chan, C.; Ruehter, G. *J. Am. Chem. Soc.* **1997**, *119*, 698−708.
(24) Trost, B. M.; Chan, C.; Ruhter, G. *J. Am. Chem. Soc.* **1987**, *109*, 3486−3487.
(25) Derien, S.; Monnier, F.; Dixneuf, P. H. *Top. Organomet. Chem.* **2004**, *11*, 1−44.
(26) Musaev, D. G.; Morokuma, K. *Top. Organomet. Chem.* **2005**, *12*, 1−30.
(27) Bianchini, C.; Peruzzini, M.; Vacca, A.; Zanobini, F. *Organometallics* **1991**, *10*, 3697−707.
(28) Bruce, M. I. *Chem. Rev.* **1991**, *91*, 197−257.
(29) Perez-Carreno, E.; Paoli, P.; Ienco, A.; Mealli, C. *Eur. J. Inorg. Chem.* **1999**, 1315−1324.
(30) Bruneau, C.; Dixneuf, P. H. *Acc. Chem. Res.* **1999**, *32*, 311−323.
(31) Grotjahn, D. B.; Zeng, X.; Cooksy Andrew, L. *J. Am. Chem. Soc.* **2006**, *128*, 2798−2799.
(32) Herberich, G. E.; Barlage, W. *Organometallics* **1987**, *6*, 1924−1930.
(33) Bassetti, M.; Casellato, P.; Gamasa, M. P.; Gimeno, J.; Gonzalez-Bernardo, C.; Martin-Vaca, B. *Organometallics* **1997**, *16*, 5470−5477.
(34) Frohnapfel, D. S.; White, P. S.; Templeton, J. L. *Organometallics* **2000**, *19*, 1497−1506.
(35) Bassetti, M.; Marini, S.; Diaz, J.; Gamasa, M. P.; Gimeno, J.; Rodriguez-Alvarez, Y.; Garcia-Granda, S. *Organometallics* **2002**, *21*, 4815−4822.
(36) Gao, Y.; Jennings, M. C.; Puddephatt, R. J. *J. Chem. Soc., Dalton Trans.* **2003**, 261−265.
(37) Navarro, J.; Sola, E.; Martin, M.; Dobrinovitch, I. T.; Lahoz, F. J.; Oro, L. A. *Organometallics* **2004**, *23*, 1908−1917.
(38) Hirabayashi, T.; Sakaguchi, S.; Ishii, Y. *Adv. Synth. Catal.* **2005**, *347*, 872−876.
(39) (a) Marchenko, A. V.; Gerard, H.; Eisenstein, O.; Caulton, K. G. *New J. Chem.* **2001**, *25*, 1244−1255. (b) Marchenko, A. V.; Gerard, H.; Eisenstein, O.; Caulton, K. G. *New J. Chem.* **2001**, *25*, 1382−1388.
(40) Morales-Morales, D.; Redon, R.; Wang, Z.; Lee, D. W.; Yung, C.; Magnuson, K.; Jensen, C. M. *Can. J. Chem.* **2001**, *79*, 823−829.

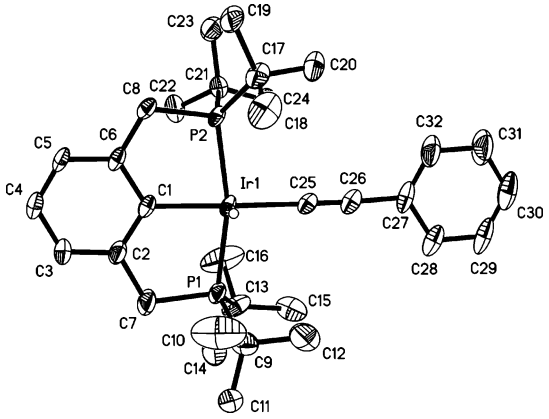

Figure 2. X-ray structure of (PCP)Ir(H)(CCPh) (**3**) with thermal ellipsoids shown at 50% thermal probability. Only one of two inequivalent molecules per asymmetric unit is shown.

lographic value for the free enyne (1.21 Å) and in the range of other acetylenes coordinated to neutral iridium(I) centers.[41]

Although the dimerization does not proceed catalytically (for reasons that will be discussed below), eq 2 is clearly relevant to several late-transition-metal systems which do catalyze phenylacetylene dimerization in some cases to give, predominantly or exclusively, enynes of the same regio- and stereochemistry as **2**.[10,13−17] Prompted by our interest in the formation of C−C bonds via C−H activation, we undertook a mechanistic study of reaction 2.

2. Addition of the Alkynyl C−H Bond. Addition of a single equiv of phenylacetylene to (PCP)Ir(NBE) results in the immediate clean formation of a single product (**3**) as indicated by ^{31}P NMR spectroscopy (δ 72.3 ppm).

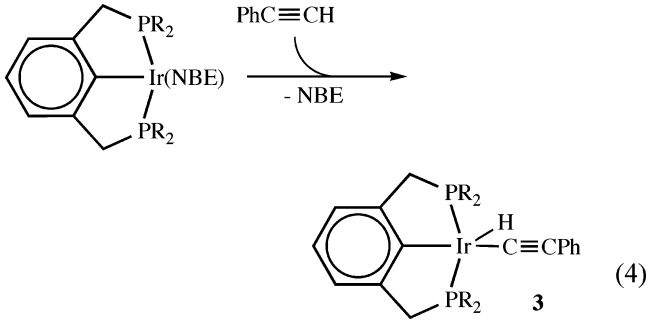

(4)

The ^{1}H NMR spectrum, in particular the strongly upfield signal at δ −43.48 ppm, is indicative of a five-coordinate Ir(III) complex with H trans to a vacant coordination site. The spectral features attributable to the *t*-butyl and methylene protons indicate that the molecule has only C_s symmetry. These observations indicated that **3** is the product of addition of the phenylacetylene alkynyl C−H bond to (PCP)Ir. Crystals of **3** were obtained by slow evaporation of a hexane solution of the compound. X-ray diffraction confirmed its spectroscopic characterization as the phenylacetylene C−H addition product; an ORTEP diagram is shown in Figure 2.

Five-coordinate products of aryl and vinyl C−H bond addition to (PCP)Ir have been previously reported.[42] (PCP)Ir(H)(Ph) and related aryl (and vinyl) hydride complexes have been found to undergo rapid (NMR time scale) exchange with free arene, at temperatures as low as −40 °C, via a dissociative pathway (as determined by dynamic NMR kinetics experiments). Consistent with a dissociative exchange pathway, no H/D exchange between arenes is observed to be effected by (PCP)Ir(aryl)(H) complexes. For example, the rapid equilibrium shown in eq 5 is observed in a solution of C_6D_6 and toluene-d_0.[42] Thus, less than 1 of every ca. 10^6 arene/arene exchange events results in H/D exchange.

$$(\mathrm{PCP})\mathrm{Ir}(\mathrm{C_6D_5})(\mathrm{D}) + \text{toluene-}d_0 \rightleftharpoons (\mathrm{PCP})\mathrm{Ir}(\text{tolyl})(\mathrm{H})\ (\text{isomers}) + \mathrm{C_6D_6} \quad (5)$$

In contrast to the aryl hydride analogues, the NMR spectrum of **3** is that of a nonfluxional complex even at 90 °C, thus alkynyl C−H elimination is orders of magnitude slower than elimination of aryl or vinyl C−H bonds. This suggests that addition of the alkynyl C−H bond is much more favorable than addition of a phenyl C−H bond. Accordingly, the addition of phenylacetylene (1.0 equiv) to a benzene solution of (PCP)-IrPhH results in complete conversion to complex **3**.

$$(\mathrm{PCP})\mathrm{Ir}(\mathrm{H})(\mathrm{Ph}) + \mathrm{HCCPh} \rightleftharpoons (\mathrm{PCP})\mathrm{Ir}(\mathrm{H})(\mathrm{CCPh})\ (\mathbf{3}) + \mathrm{PhH} \quad (6)$$

As the equilibrium of eq 6 lies too far to the right to be measured, even in benzene solution, we obtain a lower limit, $K_6 > 10^4$, corresponding to $\Delta G < -5.4$ kcal/mol. If we approximate $\Delta S = 0$, then $\Delta H < -5.4$ kcal/mol. Since the alkynyl C−H bond is ca. 18 kcal/mol stronger than the phenyl-H bond,[43,44] it follows that the Ir−CCPh bond of **3** is at least 23 kcal/mol stronger than the Ir−Ph bond of (PCP)IrPhH. Density-functional theory (DFT) calculations (discussed in section 8) indicate that the difference is even greater; reaction 6 is calculated to be exoergic by 28.6 kcal/mol. Direct calculation of bond dissociation energies (BDEs) from consideration of the proper homolytic bond-cleavage reactions leads to the following Ir−C and H−C values (kcal/mol): Ir−CCPh = 114.0, Ir−C(Ph) = 72.1, H−CCPh = 124.5, and H−C(Ph) = 108.2. Thus, the computed Ir−CCPh BDE is substantial and about 42 kcal/mol greater than that of the Ir−C(Ph) bond.

Although **3** is nonfluxional on the NMR time scale, it does undergo alkyne/alkyne exchange within minutes of mixing at room temperature. When PhCCD is added to a solution of ^{13}C labeled **3**, (PCP)Ir(^{13}CCPh)(H), full isotopic scrambling is observed according to the equilibrium of eq 7.

$$(\mathrm{PCP})\mathrm{Ir}(^{13}\mathrm{CCPh})(\mathrm{H}) + \mathrm{DCCPh} \rightleftharpoons (\mathrm{PCP})\mathrm{Ir}(\mathrm{CCPh})(\mathrm{D}) + \mathrm{H}^{13}\mathrm{CCPh} \rightleftharpoons (\mathrm{PCP})\mathrm{Ir}(^{13}\mathrm{CCPh})(\mathrm{D}) + \mathrm{HCCPh} \rightleftharpoons (\mathrm{PCP})\mathrm{Ir}(\mathrm{CCPh})(\mathrm{H}) + \mathrm{D}^{13}\mathrm{CCPh} \quad (7)$$

Thus, in spite of a much slower rate of alkyne/alkyne exchange as compared with the arene/arene exchange reactions of (PCP)Ir(H)(aryl), H/D exchange is much faster for the alkynyl hydride **3**. The isotopic exchange is suggestive of an associative mechanism for alkyne/alkyne exchange. Such a mechanism

(41) (a) Calabrese, J. C.; Roe, D. C.; Thorn, D. L.; Tulip, T. H. *Organometallics* **1984**, *3*, 1223−1230. (b) Grotjahn, D. B.; Hoerter, J. M.; Hubbard, J. L. *J. Am. Chem. Soc.* **2004**, *126*, 8866−8867.
(42) Kanzelberger, M.; Singh, B.; Czerw, M.; Krogh-Jespersen, K.; Goldman, A. S. *J. Am. Chem. Soc.* **2000**, *122*, 11017−11018.
(43) Barckholtz, C.; Barckholtz, T. A.; Hadad, C. M. *J. Am. Chem. Soc.* **1999**, *121*, 491−500.
(44) Ervin, K. M.; Gronert, S.; Barlow, S. E.; Gilles, M. K.; Harrison, A. G.; Bierbaum, V. M.; DePuy, C. H.; Lineberger, W. C.; Ellison, G. B. *J. Am. Chem. Soc.* **1990**, *112*, 5750−5759.

could proceed, inter alia, through an Ir(V) intermediate,[45] an Ir(V) transition state (or oxidative hydrogen migration),[46] or a concerted σ-bond metathesis pathway.

3. Insertion of Phenylacetylene into Ir−H Bonds. Addition of 1 equiv phenylacetylene to a benzene solution of acetylide complex **3** at room-temperature results in the rapid formation of two new species, **4a** and **4b**, with ^{31}P NMR chemical shifts of δ 36.8 and 36.5 ppm, respectively. No hydride peaks are present in the ^{1}H NMR spectrum, which does reveal two sets of triplets possibly attributable to the protons of two (PCP)Ir-bound vinyl groups; one set appears at 4.35 and 4.39 ppm, while the second set is observed at 4.79 and 6.65 ppm. ^{31}P-^{1}H hetero-COSY revealed that the first set correlates to the ^{31}P NMR peak at 36.8 ppm, and the second set correlates to the peak at 36.5 ppm. No cross correlation is observed between these two sets of peaks in the ^{1}H COSY spectrum. The spectral data are consistent with the assignment of the two species as products of insertion of the PhCCH triple bond into the Ir−H bond of **3**, to give two rotamers, as indicated in eq 8.

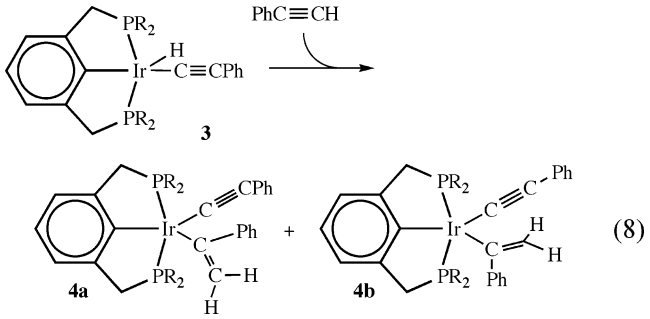

(8)

The large difference in the chemical shift of the vinylic protons of **4b** is consistent with the proximity of one proton to the acetylide group, a well-precedented effect attributed to the magnetic susceptibility of the triple bond.[47]

When complexes **4a** and **4b** are prepared from the reaction of (PCP)Ir(NBE) with 2 equiv PhC^{13}CH, their ^{13}C NMR spectroscopic parameters are found to be quite similar but with one notable difference: a ^{13}C-^{13}C coupling constant of 7.6 Hz is observed for the isotopically enriched positions of **4b**, whereas *no* such coupling is observable for **4a**. The assignment of **4a** and **4b** as indicated in eq 8 was strongly supported by DFT calculations (discussed in detail in section 8); the spin−spin couplings between the acetylide-α-C and vinyl-β-C nuclei were calculated as 9.5 and 0.5 Hz for **4b** and **4a**, respectively. Thus, this surprisingly large difference (for which we have no qualitative explanation) was very well captured by the calculations.

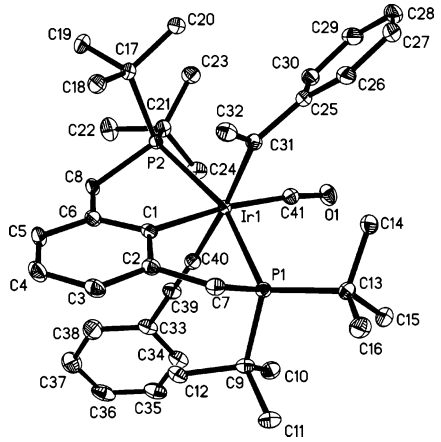

Figure 3. X-ray structure of (PCP)Ir(PhC=CH$_2$)(CCPh)(CO) (**4-CO**) with thermal ellipsoids shown at 50% thermal probability.

Addition of CO (1 atm) to a **4a**/**4b** mixture at room-temperature results in a *single* CO addition product, **4-CO**. Complex **4-CO** was crystallized by slow evaporation of a hexane solution. X-ray diffraction reveals that **4-CO** has the rotational conformation (CH_2 group syn to PCP aryl) assigned to **4a** (Figure 3). When CO (1.7 atm) was added to a **4a**/**4b** mixture at −35 °C, all **4a** was immediately converted to **4-CO**, *but **4b** remained unreacted*. Slowly warming the solution to 20 °C eventually resulted in the disappearance of **4b** and complete conversion to **4-CO**. These results clearly offer further support to the assignment of **4a** and **4b** as the iridium(1-phenylvinyl)(2-phenylacetylide) complexes, and in particular as the respective rotamers indicated in eqs 8 and 9.

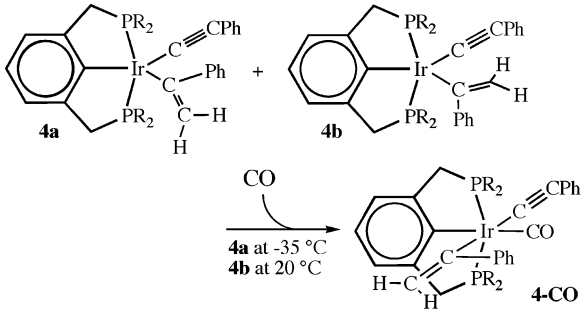

(9)

The formation of complexes **4a** and **4b** was an unexpected result, given that the ultimate product of (PCP)Ir with 2 equiv of PhCCH is the 1,4-diphenyl-butyne-ene adduct, **1**. As indicated in Scheme 1, PhCCH insertion into the Ir−H bond is, a priori, a plausible first step toward that product; however, the regiochemistry of the observed insertion is inconsistent with the mechanism of Scheme 1, since C−C elimination would give 1,3-diphenyl-butyne-ene.

The observed "wrong" regiochemistry of the PhCCH insertion (a 1,2-addition), to give **4a** and **4b**, is offset by an even more surprising result. The acetylene insertion reaction of eq 8 is found to be *reversible*, yielding easily detected equilibrium concentrations of **3**, **4a**, **4b**, and phenylacetylene. Thus, the observed 1,2-addition, to give **4a** and **4b**, is presumably a dead-end on the pathway to complex **1.**

To our knowledge there are no reported precedents of a well-characterized reversible insertion of an alkyne into a metal−H bond, or, even more generally, β-H elimination from a metal−vinyl complex to give a simple metal hydride. Perhaps the only

(45) (a) Klei, S. R.; Tilley, T. D.; Bergman, R. G. *J. Am. Chem. Soc.* **2000**, *122*, 1816−1817. (b) Kawamura, K.; Hartwig, J. F. *J. Am. Chem. Soc.* **2001**, *123*, 8422−8423. (c) Mohammad, H. A. Y.; Grimm, J. C.; Eichele, K.; Mack, H.-G.; Speiser, B.; Novak, F.; Quintanilla, M. G.; Kaska, W. C.; Mayer, H. A. *Organometallics* **2002**, *21*, 5775−5784. (d) Krogh-Jespersen, K.; Czerw, M.; Summa, N.; Renkema, K. B.; Achord, P. D.; Goldman, A. S. *J. Am. Chem. Soc.* **2002**, *124*, 11404−11416. (e) Webster, C. E.; Hall, M. B. *Coord. Chem. Rev.* **2003**, *238*−239; 315−331. (f) Lam, W. H.; Lam, K. C.; Lin, Z.; Shimada, S.; Perutz, R. N.; Marder, T. B. *J. Chem. Soc., Dalton Trans.* **2004**, 1556−1562. (g) Bernskoetter, W. H.; Lobkovsky, E.; Chirik, P. J. *Organometallics* **2005**, *24*, 4367−4373.

(46) (a) Oxgaard, J.; Muller, R. P.; Goddard, W. A.; Periana, R. A. *J. Am. Chem. Soc.* **2004**, *126*, 352−363. (b) Oxgaard, J.; Periana, R. A.; Goddard, W. A., III. *J. Am. Chem. Soc.* **2004**, *126*, 11658−11665.

(47) (a) Agarwal, A.; McGlinchey, M. J. *Can. J. Chem.* **1978**, *56*, 959−961. (b) Alkorta, I.; Elguero, J. *New J. Chem.* **1998**, *22*, 381−385. (c) Abraham, R. J.; Reid, M. *J. Chem. Soc., Perkin Trans.* **2001**, *2*, 1195−1204. (d) Martin, N. H.; Nance, K. H. *J. Mol. Graphics Modell.* **2002**, *21*, 51−56.

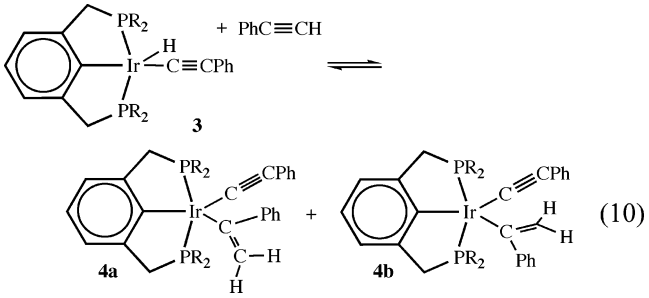

(10)

well characterized example of alkyne deinsertion from a metal−vinyl group was reported by Puddephatt.[36] In that case, an equilibrium was observed and measured; however, the product was a bridging hydride and the formation of such a bridge must obviously affect the thermodynamics to some degree.

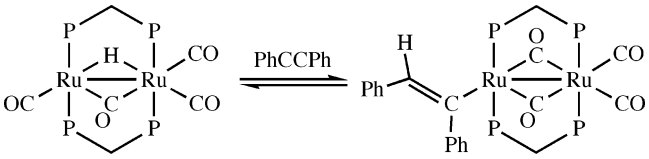

To further investigate the novel equilibrium of eq 10, the temperature dependence was determined from 25 up to 45 °C at intervals of 5 °C (and then back down to 25 °C at the same intervals to confirm that the observed concentrations were in fact equilibrium values). Plots of $R \ln K$ versus $1/T$ (Figure 4) yielded the following values of ΔH and ΔS: for formation of **4a**, −15.4(5) kcal mol^{-1} and −38.9(16) cal deg^{-1} mol^{-1}, and for formation of **4b**, −13.9(4) kcal mol^{-1} and −37.0(14) cal deg^{-1} mol^{-1}. These very negative entropy values are consistent with the formation of a highly crowded species in which numerous low-frequency vibrational modes are restricted, relative to complex **3** and free phenylacetylene.

At −35 °C, the reaction of complex **3** (37 mM) with 1.5 equiv of phenylacetylene gave complex **4a** exclusively; the conversion of **3** to **4a** is observed to be essentially complete in approximately 45 min. This result is consistent with DFT calculations (discussed in detail in section 8), which show that the most favorable approach of the incoming acetylene is a vacant coordination site trans to the PCP iridium-bound carbon. Such an approach would yield the rotameric form **4a**, as indicated in Figure 5. Warming the resulting solution of **4a** to room-temperature yields a mixture of **4a** and **4b** (in the same ratio, 1:0.6, as obtained when PhCCH is added to **3** at room temperature).

The kinetic data was fit using the program Gepasi[48] to give the rate constants 1.08(9) × 10^{-1} M^{-1} s^{-1} for $k_{11(4a)}$ (insertion) and 1.3(3) × 10^{-4} s^{-1} for $k_{-11(4a)}$ (β-H elimination). These rates correspond to activation free energies (−35 °C) of 14.9 kcal/mol and 18.1 kcal/mol, respectively.

Further investigation of the reactivity of PhCCH with iridium hydride complexes was conducted with (PCP)IrHCl. As in the case of the reaction with hydride **3**, insertion occurred, and with complete regioselectivity. Quite surprisingly, however, in the case of (PCP)IrHCl, the only insertion product observed was the result of the reverse regioselectivity, that is, 2,1-insertion.

(48) (a) Mendes, P. *Comput. Appl. Biosci.* **1993**, *9*, 563−571. (b) Mendes, P. *Trends Biochem. Sci.* **1997**, *22*, 361−363. (c) Mendes, P.; Kell, D. *Bioinformatics* (Oxford) **1998**, *14*, 869−883.

Complex **5** was characterized by ^{1}H and ^{31}P NMR; particularly diagnostic are the vinyl proton signals, which are broad peaks at δ 8.60 and δ 4.65 ppm, with J_{HH} = 13.5 Hz. A closely related vinyl complex, in which an analogous α-vinyl proton resonates at δ 8.22 ppm, has been reported by Crabtree.[20]

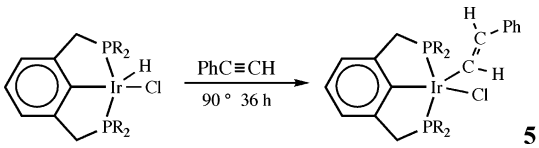

(11)

Complex **5** was difficult to obtain in pure form but addition of CO atmosphere to a solution of complex **5** gave the CO adduct, **5-CO**, which was successfully purified by column chromatography.

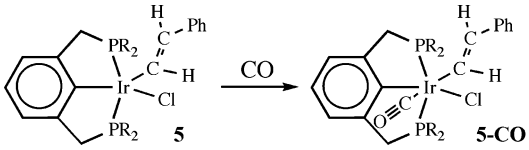

(12)

The ^{1}H and ^{31}P NMR parameters of **5-CO** were similar to that of **5** (δ 8.73 ppm, J_{HH} = 18.2 Hz, J_{HP} = 2.2 Hz; δ 5.83 ppm, J_{HH} = 18.2 Hz, J_{HP} = 2.2 Hz). The complex was recrystallized from 25% hexane in benzene, and its structure was crystallographically determined (Figure 6).

We further exploited the ability to obtain pure samples of the CO adduct. Complex **5-CO** was synthesized from the reaction of (impure) **5** with CO. Following column chromatography, it was reacted with trimethylamine oxide to give back complex **5**, which was then recrystallized from hexane solution. The structure of **5** was confirmed by crystallography (Figure 6).

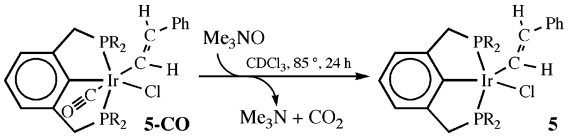

(13)

The kinetic barrier to the insertion reaction of eq 11 is significantly greater than that of reaction 8 (insertion of PhCCH into the Ir−H bond of **3**). Reaction 11 proceeds slowly at 90 °C (approximately 2 × 10^{-4} M^{-1} s^{-1}), as compared with reaction 8 which is relatively fast at −35 °C (1.08(9) × 10^{-1} M^{-1} s^{-1}). While reaction 11 does not proceed cleanly, giving only about a 40% NMR yield of **5** (the remaining products were unstable to chromatography and not characterized), the ^{1}H NMR spectrum of the product solution (vinyl H region) reveals the absence of any significant quantity of the 1,2-insertion product. Since we see no reason why the kinetic regioselectivity of addition would be completely reversed for (PCP)IrHCl versus (PCP)IrH(CCPh), we suspect that 1,2-addition is also kinetically favorable for (PCP)IrHCl, but reversible, and that the 2,1-addition product is the thermodynamic sink (probably more favorable owing to steric effects).

To summarize this section, PhCCH inserts readily into the Ir−H bond of **3**, as required by the Ir−H addition pathway of Scheme 1. However, the 1,2 regiochemistry of the insertion is *inconsistent* with this pathway. But the insertion is easily reversible (which represents an unprecedented example of simple

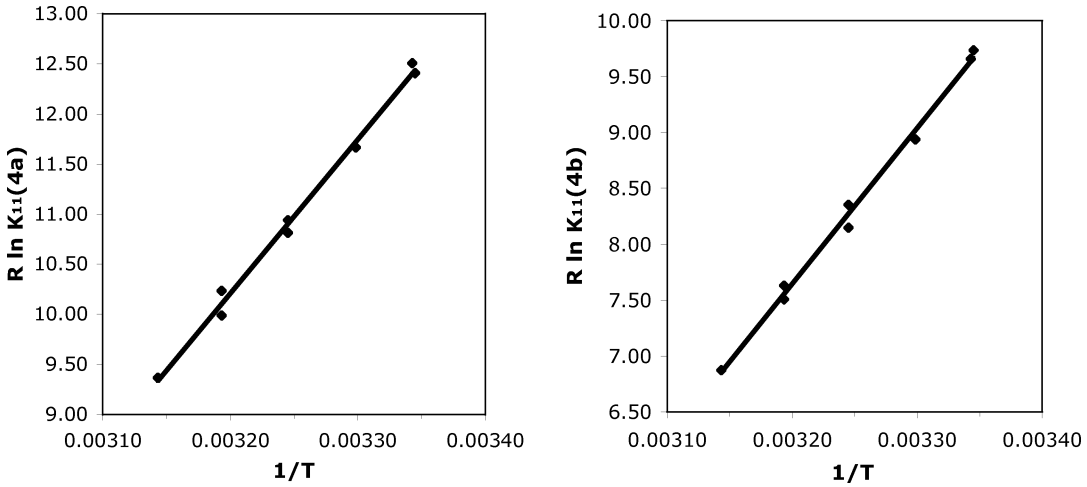

Figure 4. Equilibrium plots for the reversible insertion of phenylacetylene (eq 10): formation of complex **4a** and formation of complex **4b**.

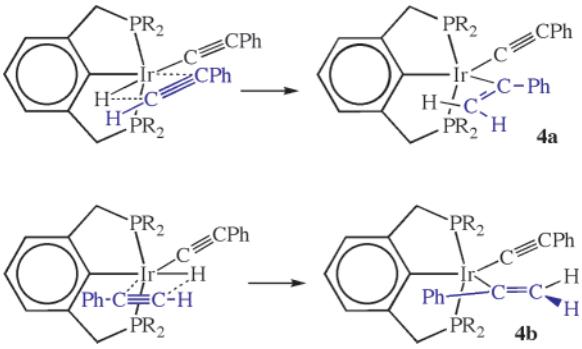

Figure 5. Two possible approaches of a phenylacetylene molecule for 1,2-insertion into the Ir−H bond of **3**. Without rotation around the resulting Ir−C bond, each approach can yield one of the two isomer/rotamers of **4**.

β-H elimination from a transition-metal vinyl complex), and it presumably does not play a role in the formation of the 1,4-diphenylbutene-yne product. Interestingly, PhCCH inserts into the Ir−H bond of (PCP)IrHCl to give exclusively the product of 2,1-insertion.

4. C−C Elimination To Give Complex 1. In the context of the mechanism of eq 2, the reversible 1,2-insertion of PhCCH into the Ir−H bond of **3** presumably represents an out-of-cycle dead end. In that respect the two pathways of Scheme 1, Ir−H addition and Ir−C addition, are equally consistent with this insertion reaction. The very low barrier to the 1,2-insertion ($\Delta G^{\ddagger} \approx 15$ kcal/mol), however, suggested to us that the 2,1-insertion (i.e., the regioselectivity consistent with the observed product) was likely to be at least facile enough to be consistent with the overall kinetics of reaction 2. This suspicion was supported by the observation that the reaction of PhCCH with (PCP)IrHCl gave exclusively the 2,1-insertion product; thus the barrier to a 2,1-insertion into a (PCP)IrH bond is not necessarily prohibitively high.

With this hypothesis in mind, we attempted an independent synthesis of the product that would result from the 2,1-insertion of PhCCH into the Ir−H bond of **3**. Complex **5** was reacted with 2.5 equiv lithium arylacetylide (1 M solution in THF) to yield the desired iridium(acetylide)vinyl complex, **6**, in 92% yield (eq 14; Ar = tolyl). Lithium *p*-tolylacetylide (rather than phenylacetylide) was used to aid in NMR characterization, and to confirm the origin of the acetylide group in product **6** and in any subsequent elimination reactions.

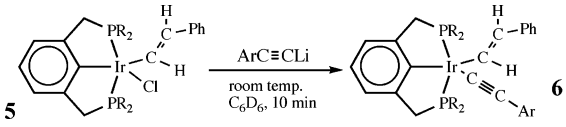

(14)

Addition of CO to a benzene solution of **6** yields the carbonyl adduct **6-CO**. Crystals of **6-CO** were obtained from pentane, and its structure was determined by crystallography (Figure 7).

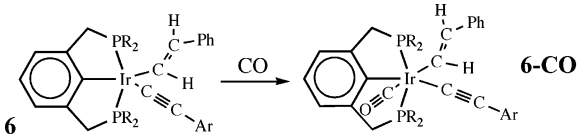

(15)

Complex **6** (Ar = Ph) is isomeric with complexes **4a** and **4b**, with a phenyl on the vinylic β-carbon (trans to Ir) rather than the α-carbon. Complex **6** is therefore presumably less crowded than **4a** and **4b** which do not undergo C−C elimination. Thus, a priori, it would be expected that **6** would also not undergo C−C elimination. *In fact, in striking contrast with the behavior of **4**, complex **6** does undergo facile, and clean, C−C bond elimination* to yield complex **1**.

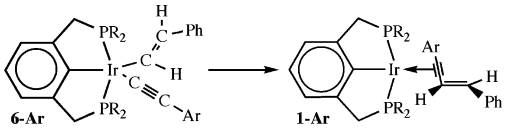

(16)

At 40 °C, the rate constant of reaction 16 (Ar = Ph) is $3.1(5) \times 10^{-4}$ s^{-1} (corresponding to $\Delta G^{\ddagger} = 23.4$ kcal/mol; Figure 8). (It should be noted that it was possible to remove from solution most, but not all, excess THF from the solution in which **6** was generated; continued efforts to remove all THF were accompanied by loss of **6**. Residual THF concentrations varied, which did not affect the rate of eq 16. However, we cannot rigorously exclude the possibility that coordination of THF could be inhibiting C−C elimination;[49] in that case the intrinsic difference between the C−C elimination rates of complex **6** and complexes **4** would be even greater than these results indicate.)

(49) (a) Crumpton, D. M.; Goldberg, K. I. *J. Am. Chem. Soc.* **2000**, *122*, 962−963. (b) Crumpton-Bregel, D. M.; Goldberg, K. I. *J. Am. Chem. Soc.* **2003**, *125*, 9442−9456 and references therein.

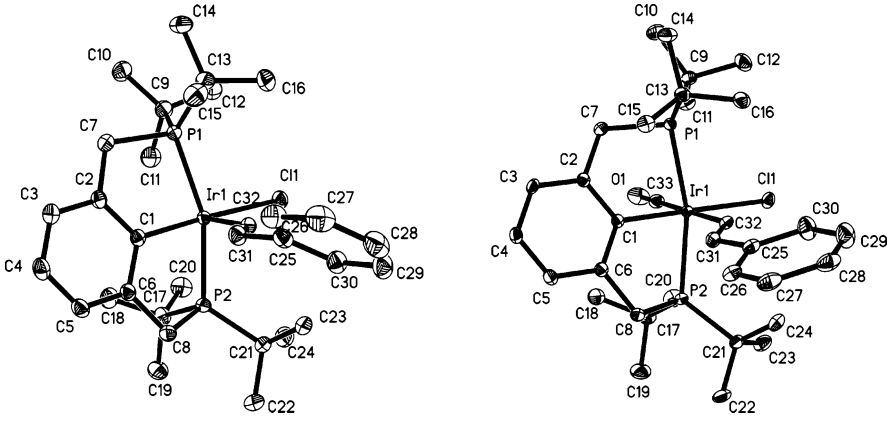

Figure 6. X-ray structures of (PCP)Ir(CH═CHPh)(Cl) (**5**) and (PCP)Ir(CH═CHPh)(Cl)(CO) (**5-CO**) with thermal ellipsoids shown at 50% thermal probability.

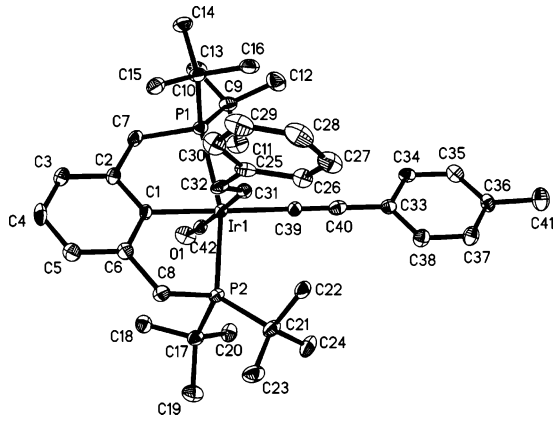

Figure 7. X-ray structure of (PCP)Ir(CO)(CH═CHPh)[CC(*p*-tol)] (**6-CO**; Ar = *o*-Tol) with thermal ellipsoids shown at 50% thermal probability.

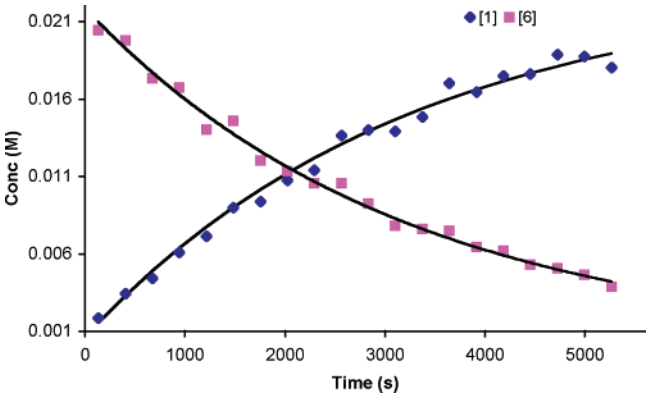

Figure 8. Kinetics of eq 16, C−C reductive elimination from **6** (Ar = Ph), at 40 °C. Lines shown are theoretical first-order fits.

Consistent with an intramolecular mechanism for C−C elimination from complex **6**, the kinetics of eq 16 are first order (Figure 8) while the coordinated enyne of complex **1-tol** has a tolyl group at the acetylide position and a phenyl group bound to the vinylic carbon (as shown in eq 16). The ^{1}H NMR spectrum of the enyne has a single signal attributable to a *p*-methyl group, at δ 1.91 ppm, which corresponds to the methyl on the phenylacetylenyl unit; the *p*-methyl on the styrenyl unit appears at δ 1.95 ppm (see Supporting Information for full characterization).[50]

The results discussed above and in preceding sections strongly implicate the Ir−H insertion pathway (Scheme 1) as the mechanism of eq 2. In particular (i) C−H addition to give complex **3** (eq 4) is observed to occur rapidly upon addition of PhCCH to (PCP)Ir(NBE); (ii) insertion of PhCCH into the Ir−H bond of **3** occurs rapidly, with the wrong regioselectivity (1,2 insertion) to lead to complex **2**; however, this reaction is readily reversible; (iii) insertion of PhCCH into the Ir−H bond of (PCP)IrHCl occurs (slowly) to give exclusively the 2,1-insertion product; thus, in a species closely related to **3**, the barrier to 2,1-insertion is high, but not prohibitively so; (iv) most importantly, complex **6**, the putative product of a 2,1-insertion of PhCCH into the Ir−H bond of **3**, undergoes C−C elimination to give **1**, with a rate faster than that of the overall reaction of eq 2; that is, **6** is a kinetically competent intermediate.

5. Kinetics of Enyne Formation. Kinetics of the reaction of acetylide hydride **3** (85 mM) with 2 equiv phenylacetylene, to give enyne complex **1**, were monitored at 40 °C by ^{31}P NMR. The data obtained was fit using Gepasi[48] (Figure 9) using a scheme (Scheme 2) which involves reversible formation of complex **4a** and **4b** (in equilibrium, *K*) and the relatively slow formation of complex **6** which subsequently transforms to complex **1**. The rate constant for the formation of complex **6** (k_3) was thereby determined to be $1.04(6) \times 10^{-2}$ M^{-1} s^{-1}. The quality of the fit was less sensitive to the values of rate constants other than k_3, which are therefore less reliable: $k_1 = 2.7$ M^{-1} s^{-1}, $k_{-1} = 3.7 \times 10^{-2}$ s^{-1}, $k_2 = 5.5 \times 10^{-1}$ M^{-1} s^{-1}, $k_{-2} = 1.3 \times 10^{-2}$ s^{-1}, $k_4 = 1.4 \times 10^{-3}$ s^{-1}, $k_5 = 1.4 \times 10^{-4}$ M^{-1} s^{-1} (k_5 refers to a secondary reaction of **1** with PhCCH; see below).[51]

The failure to observe any 1,3-diphenyl-but-3-ene-1-yne permits us to extrapolate an upper limit for the rate of C−C bond elimination from **4a** or **4b**. By estimating a 2% detection limit, we can obtain an upper limit of 3×10^{-6} s^{-1} for elimination from **4a**, or 5×10^{-6} s^{-1} for elimination from **4b**. These values correspond to lower limits, of the activation free energies of elimination, of 26.3 kcal/mol and 26.0 kcal/mol, respectively.

6. C−C Elimination: Further Studies. Although, from the outset of this investigation, we had considered the pathway

(50) The trend of the *p*-methyl on the styrenyl being deshielded as compared to the *p*-methyl on the phenylacetylene is seen in *trans*-1-(4-tolyl)-prop-1-ene: Yu, J.; Gaunt, M.J.; Spencer, J. B. *J. Org. Chem.* **2002**, *67*, 4627−4629. Seen in 1-(4-methylphenyl)-prop-1-yne: Weiss, H. M.; Touchette, K. M.; Angell, S.; Khan, J. *Org. Biomol. Chem.* **2003**, *1*, 2152−2156.

(51) The value chosen for k_1 was extrapolated to 40 °C from the value determined experimentally at −35 °C, by assuming an entropy of −39 eu (the thermodynamic entropy of insertion). The value of k_{-1} then gave a best fit consistent with the observed equilibrium, K_1. Since the reactions corresponding to k_1, k_{-1}, k_2, and k_{-2} are fast relative to k_3, only the ratios (i.e. K_1 and K_2) were constrained by the data.

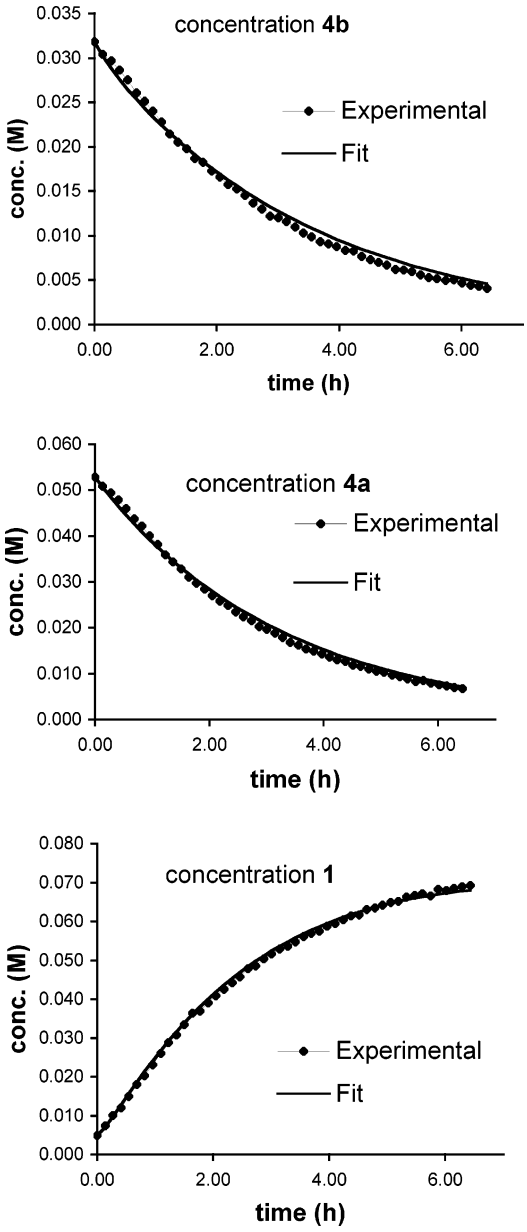

Figure 9. Kinetic fits for the formation of enyne complex **1** from the reaction of acetylide hydride **3** with phenylacetylene. (Note that most of **3** is rapidly converted to an equilibrium concentration of **4a** and **4b** prior to the first data point.)

leading to product as shown in Scheme 2 to be very plausible, the above results present a very surprising conclusion: the regioselectivity of eq 2 is determined by the C−C elimination rather than by the Ir−H addition step. Ir−H addition occurs preferentially in the "wrong" (1,2) direction; however, only the product of the much less favorable (2,1) addition reaction undergoes C−C elimination. This completely unanticipated conclusion is all the more surprising because the more easily formed insertion isomer is the *more* crowded one (**4**), but this one does not undergo reductive elimination. In view of the profound importance of C−C elimination in organometallic and organic chemistry, this conclusion clearly merited further study.

The reaction of 1-phenylpropyne (PhCCMe) with complex **3** (50 °C, ca. 30 min) yields complexes **7a** and **7b**, in a ratio of 1.1:1. Complex **7a** has been crystallographically characterized as the product of 2,1 addition of Ir−H across the acetylene triple bond (i.e., the product with phenyl bound to the β-vinyl carbon; Figure 10 and eq 17). On the basis of its ^{1}H and ^{31}P NMR spectral data, complex **7b** is proposed to be an Ir−C rotamer of **7a**, in analogy with the phenylacetylene insertion products **4a** and **4b**. It is not clear if formation of **7a** and **7b** (the 2,1 addition products) are kinetically favored over 1,2-addition products; in view of the results obtained with phenylacetylene, it seems entirely plausible that the 1,2 addition is kinetically favored, but reversible, while complexes **7a** and **7b** constitute the thermodynamic sink.

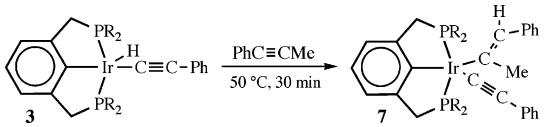

(17)

In contrast with the closely related β-phenylvinyl complex **6**, complex **7** shows no indication of undergoing C−C elimination. Complex **7** is stable up to ca. 60 °C (in contrast with **6**, which undergoes rapid C−C elimination at 40 °C, eq 16); at 70 °C, it undergoes conversion to give products resulting from a complex rearrangement. This rearrangement is beyond the scope of this paper; the important point is that the presence of the methyl substituent on the vinyl group precludes vinyl-alkynyl C−C elimination from **7**, even at 70 °C.

In the course of this work, one other complex of the type (PCP)Ir(CCPh)(CR═CHR′) was isolated. As noted above, the formation of enyne **2** is not catalytic. Apparently, this is *not* because the enyne is bound too strongly to be displaced. Instead, if more than 2 equiv phenylacetylene are added to a solution of (PCP)Ir(NBE), the formation of secondary products are observed including one complex, **8**, with a ^{31}P NMR signal at 41.6 ppm. This complex could be synthesized in almost quantitative yield by treatment of complex **3** with independently synthesized enyne

Scheme 2

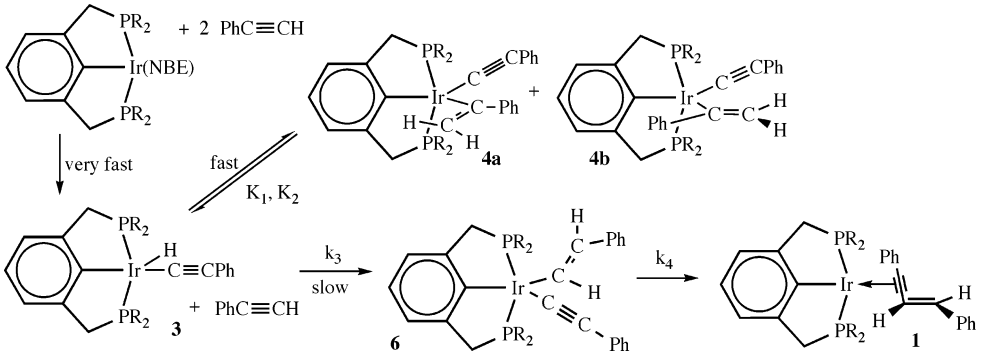

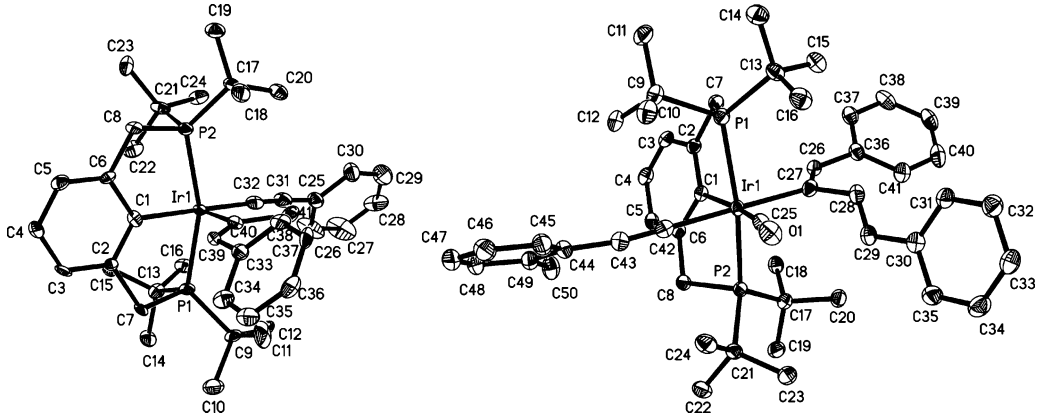

Figure 10. X-ray structures of (PCP)Ir[C(Me)═CHPh](CCPh) (**7a**) and (PCP)Ir[C(CHCHPh)═CHPh](CCPh)(CO) (**8-CO**) with thermal ellipsoids shown at 50% thermal probability.

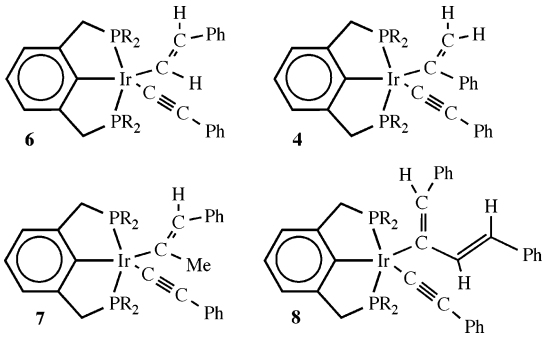

Figure 11. Characterized complexes (PCP)Ir(CCPh)(CR═CHR′)

2. The CO adduct of **8**, which appears as a broad peak at 42.6 ppm in the ^{31}P NMR spectrum, was crystallized from hexane, and its structure was determined. The structure (Figure 10) reveals that **8** is (or at least can be viewed as) the product of 2,1-addition of the Ir−H bond across the triple bond of **2** (eq 18).

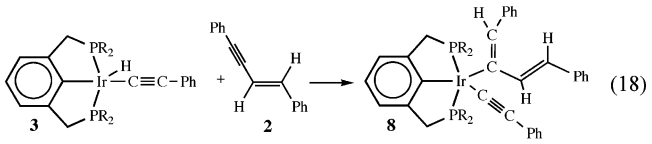

(18)

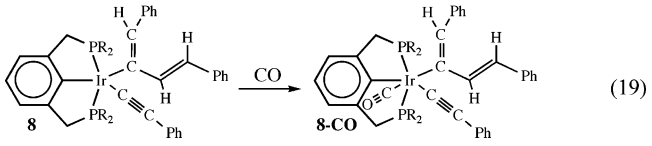

(19)

No indication of C−C elimination from complex **8** has been observed. Heating a benzene solution of **8** at 55 °C results only in slow decomposition over ca. 2 days.

Thus, we have observed and fully characterized at least four species of the formula (PCP)Ir(CCPh)(CR═CHR′) (Figure 11). Notably, only one of these complexes undergoes C−C elimination, namely **6**, which is, surprisingly, the *least* sterically hindered of the four complexes. The presence on the α-carbon of either an electron-donating substituent (methyl; complex **7**), or electron-withdrawing substituents (phenyl and vinyl; complexes **4** and **8**, respectively), inhibits C−C elimination. Therefore we must conclude that steric crowding, specifically due to the presence of substituents at the vinyl α-carbon, inhibits C−C elimination in the species shown in Figure 2. This conclusion would appear to have important potential implications for other systems in which C−C bonds (particularly with an sp^2 carbon) are formed. Insight into the origin of this effect was obtained from computational studies described below (section 8).

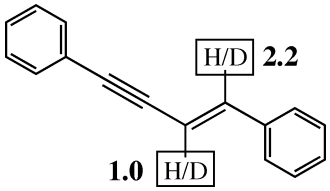

Figure 12. *trans*-1,4-Phenyl-but-3-ene-1-yne (**2**), formed from the reaction of (PCP)Ir(NBE) with PhCCH and PhCCD with isotope effects indicated.

7. Isotope Effects and Consideration of Vinylidene Pathways. Because of the rapid reaction of **3** with excess PhCCH, it was not possible to directly measure the equilibrium isotope effect for eq 20 with PhCCH/PhCCD. However, the sterically hindered alkyne 2-ethynyltoluene reacts extremely slowly with the tolyl analogue of **3**, (PCP)IrH[CC(*o*-Tol)] (**9**) (formation of the *o*-Tol analogue of enyne complex **1** has a half-life of ca. 5 days at 90 °C). The reaction of (PCP)Ir(NBE) with 1 equiv DCC(*o*-Tol) (2-ethynyl-d_1-toluene) immediately gave **9**-d_1; to this solution was added 6.6 equiv of a 1:1 mixture of DCC(*o*-Tol) and HCC(*o*-Tol). ^{1}H NMR was used to determine the ratio of **9**-d_0/**9**-d_1 as well as the ratio of HCC(*o*-Tol)/DCC(*o*-Tol), yielding a value of EIE_{20} = 1.87(5) (Ar = *o*-Tol) which we assume to be very nearly equal to that of EIE_{20} for Ar = Ph.

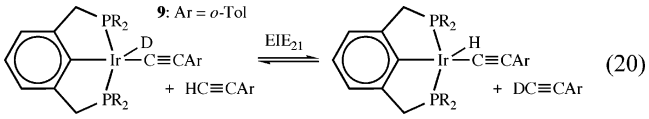

(20)

To determine the overall isotope effect for formation of the enyne complex, (PCP)Ir(NBE) was reacted with 50 equiv each of PhCCH and PhCCD, at 50 °C for 24 h. The coordinated enyne was displaced from the resulting product **1** by addition of CO to the reaction mixture. The displaced enyne **2** was isolated by column chromatography and analyzed by ^{1}H NMR and ^{2}H NMR in $CDCl_3$ and $CHCl_3$, respectively; the vinylic H/D ratios were found to be 1.0(1):1 and 2.2(1):1 at the C3 and C4 positions, respectively (Figure 12).

The H/D ratio of unity for the C3 vinylic position is expected (if secondary isotope effects are assumed to be small) for either

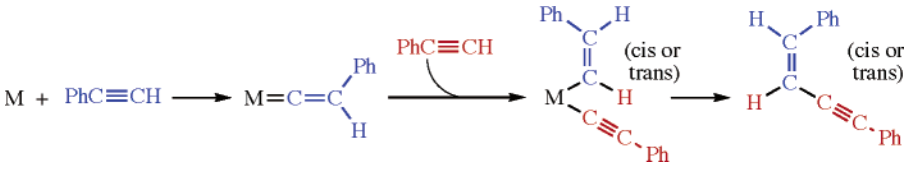

Figure 13. An a priori plausible mechanism for alkyne dimerization proceeding through vinylidene intermediates.

Table 1. Energy, Enthalpy, Entropy, and Free Energy (25 °C) Calculated (using PBE and B3LYP Functionals) for Selected Energy Minima and Transition States and Relevant Experimental Values[a]

	PBE					B3LYP		
species	*E*	*H*	*S*	*G*[b]	experimental/comments[c]	*H*	*S*	*G*
(PCP)Ir + HCCH + HCCPh	42.0	42.3	32	32.8	not observed	37.1	31	27.7
3′ + HCCPh	(0)	(0)	(0)	(0)	0	(0)	(0)	(0)
3′(*π*-PhCCH)	−3.9	−1.9	−46	11.9	not observed	9.3	−44	22.5
TS-ins-6′	9.7	9.8	−46	23.6	*G*: 21.2 (40°); 20.6 (25°)[d]	22.6	−46	36.3
TS-ins-4a′	5.7	6.1	−47	20.2	*G*: 14.9 (−35°); 17.2 (25°)[e]	18.5	−47	32.6
TS-ins-4b′	15.4	16.4	−48	30.9	no data			
4a′	−20.7	−16.6	−45	−3.2	*H*, *S*, *G*: −15.4; −39; −3.8 (25°)[f]	−8.1	−42	4.6
4b′	−19.5	−15	−48	−0.8	*H*, *S*, *G*: −13.9; −37; −2.9 (25°)[f]			
6′	−34.4	−30.8	−37	−19.7	no thermodynamic data	−23.2	−37	−12.0
TS-4a′-elim	4.8	7.7	−50	22.6	$G > 22.5$[g]	22.4	−47	36.6
TS-6′-elim	−18	−14.6	−43	−1.8	$\Delta G^{\ddagger} = 23.4$[h]			
1′	−48.6	−44.1	−37	−33.2	no thermodynamic data	−34.0	−34	−23.8
(PCP)Ir(3-Ph-enyne)[i]	−43.1	−38.3	−42	−25.6	not observed	−28.8	−35	−18.4
PCP)Ir + **2′** (free)	−10.5	−7.1	3	−7.9	not observed	−6.8	3	−7.8

[a] All values in kcal/mol except entropy (cal/(deg•mol)). [b] Free energy values; 25 °C, 1.0 M standard state. [c] Experimentally based data for corresponding observed species and transition states. [d] Obtained by fitting kinetic data (40 °C), to give $\Delta G^{\ddagger} = 21.2$ kcal/mol and then extrapolated to 25 °C, assuming $\Delta S^{\ddagger} = -38$ eu. [e] Obtained from direct kinetic measurement of eq 8 at −35 °C, to give $\Delta G^{\ddagger} = 14.9$ kcal/mol; then extrapolated to 25 °C, assuming $\Delta S^{\ddagger} = -38$ eu. [f] ΔH; ΔS; ΔG; obtained from equilibrium measurements (eq 10) over the range 25−45 °C. [g] Obtained from fitting kinetic data (40 °C) to give a lower limit for $\Delta G^{\ddagger}$ for C−C bond elimination from **4a** (26.3 kcal/mol); then adding free energy of formation of **4a** from **3** and PhCCH (−3.8 kcal/mol). [h] Obtained from direct kinetic measurement (40 °C) of the reaction of independently synthesized **6** (eq 16). [i] Isomer of complex **1′** with phenyl group at C3 rather than C4 (as would result from C−C elimination from **6′** instead of **4′**).

of the two insertion-type dimerization mechanisms indicated in Scheme 1. The H/D ratio of 2.2 found for the C4 vinylic position is larger than the value of 1.87 found for the C−H addition EIE_{20}. If secondary isotope effects are neglected, the M−C insertion pathway (assuming M−C insertion is rate-determining) would predict an H/D ratio equal to EIE_{20}. The M−H insertion pathway, however, would predict a KIE equal to the product of EIE_{20} and the KIE for insertion into the Ir−H(D) bond.

At least three distinct reaction pathways have been proposed for the catalytic hydroalkynylation of triple bonds. Two such pathways, involving C−H addition, insertion, then elimination, are indicated in Scheme 1.[19,32−38] Additionally, vinylidene mechanisms have been proposed by Werner, Crabtree, and others.[7, 10−13,20,27−31,39,52] Unlike the insertion mechanism of Scheme 1, any such vinylidene mechanism involves the cleavage of the acetylenic C−H bonds of both alkyne components (see Figure 13). Accordingly the observation of a KIE of unity for C3 argues against such a mechanism. We also note that the insertion mechanisms, but not the vinylidene mechanism, readily explain the exclusive selectivity for formation of the trans double bond geometry.

8. Computational Studies of the Full Dimerization Reaction. The full mechanism of the acetylene dimerization, proposed on the basis of experimental results discussed in the preceding sections, along with related aspects such as acetylene/acetylene exchange, was investigated computationally with the use of DFT-based electronic structure calculations. Both PBE[53] and B3LYP[54] exchange and correlation functionals were applied in the calculations; only results obtained with PBE were generally in very good agreement with experiment, and only these results will be discussed in detail here. The B3LYP functionals generally gave substantially higher energies for the more crowded species, in poor agreement with experimental data and observations (see Table 1). Most calculations were performed using the full nontruncated $^{t\text{Bu}}$PCP ligand, but changes to the dimerization energy profile resulting from the use of a truncated model pincer ligand, $^{\text{Me}}$PCP, in which *t*-butyl groups are replaced with methyls, were also investigated. Assuming that the phenyl group of the phenylacetylide ligand was too far removed from the metal center to significantly impact the dimerization reaction energies, we modeled it as a simple acetylide (CCH) ligand, while the incoming phenylacetylene molecule was not truncated. Computational models of experimental $^{t\text{Bu}}$PCP complexes (**n**) described in the preceding experimental sections, are labeled **n′**; calculated $^{\text{Me}}$PCP analogues are labeled **n″**.

8a. Insertion of Acetylene into the Ir−H Bond. Addition of the Ir−H bond of **3′** to the triple bond of phenylacetylene (i.e., insertion of phenylacetylene) is calculated to proceed with a preference for the 1,2 orientation (**TS-ins-4a′**), in accord with experiment. This preference is also calculated for **3″**, the $^{\text{Me}}$PCP complex (Figure 16); however, the difference between 1,2 and 2,1 orientations (0.7 kcal/mol) is much smaller than in the case of the full $^{t\text{Bu}}$PCP ligand (3.4 kcal/mol). This suggests

(52) Li, X.; Incarvito, C. D.; Crabtree, R. H. *J. Am. Chem. Soc.* **2003**, *125*, 3698−3699.

(53) Perdew, J. P.; Burke, K.; Ernzerhof, M. *Phys Rev. Lett.* **1996**, *77*, 3865.

(54) (a) Becke, A. D. *J. Chem. Phys.* **1993**, *98*, 5648−5652. (b) Lee, C.; Yang, W.; Parr, R. G. *Phys. Rev. B: Condens. Matter Mater. Phys.* **1988**, *37*, 785.

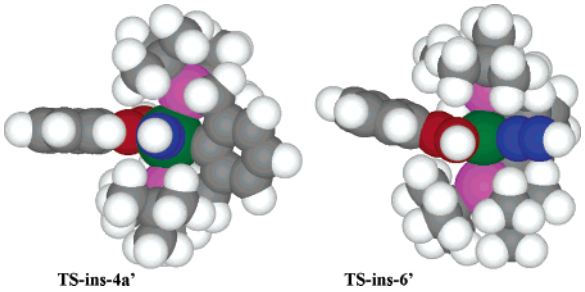

Figure 14. Calculated structures for **TS-ins-4a′** (α-phenylvinyl) and **TS-ins-6′** (*β*-phenylvinyl). The perspective is approximately as viewed down the acetylide C−C axis (atoms shown at 75% van der Waals radii; vinyl carbons in red, alkynyl carbons in blue). **TS-ins-4a′** is calculated to be 3.4 kcal/mol energetically below **TS-ins-6′**.

that the observed difference between the two orientations results largely from steric factors. This conclusion may seem counterintuitive; steric crowding might be expected to favor the TS with the phenyl group further from the iridium center. But the phosphino alkyl groups are positioned away from the site trans to the PCP carbon, and hence 1,2 insertion (**TS-ins-4a′**) may be less sterically demanding than 2,1 insertion (**TS-ins-6′**). No difference in the degree of crowding is obvious from inspection of the calculated structures, in accord with the relatively small energetic difference of 3.4 kcal/mol (see Figures 5 and 14). Note, however, when the insertion reaction is *complete*, the phenyl group is found in a much more sterically crowded position in the case of the 1,2 orientation (see below).

A 1,2-addition in which the PhCCH approaches trans to the acetylide group (**TS-ins-4b′**) was calculated to be 10.7 kcal/mol higher in activation free energy than an approach trans to the PCP aryl (**TS-ins-4a′**), in accord with the observation that **4a** is the kinetically preferred rotamer resulting from the 1,2-insertion reaction of PhCCH with **3** (see Figure 5). A 2,1 addition in which PhCCH approaches trans to the acetylide group is likewise calculated to be higher in activation free energy than a 2,1 addition approaching trans to the PCP aryl (**TS-ins-6′**); in this case, however, the difference is only 1.9 kcal/mol.

The calculated value of 17.3 kcal/mol at −35 °C (20.2 kcal/mol at 25 °C) for the 1,2-addition (to give **4a**), compares well with the experimentally determined activation free energy of 14.9 kcal/mol at −35 °C. The experimental value for the 2,1-addition, extrapolated from the overall kinetics of eq 2, is 21.2(1) kcal/mol at 40 °C. If we estimate an activation entropy of +38 eu for both addition reactions (the value determined as the *thermodynamic* entropy of the 1,2-addition), then the experimental free energy barriers at 25 °C may be estimated as 17.2 kcal/mol (1,2-addition) and 20.6 kcal/mol (2,1-addition). The difference of 3.4 kcal/mol favoring the 1,2-addition is exactly equal to the calculated difference (see Figure 15). While the level of this agreement is certainly fortuitous, the experimental and calculated differences between the two directions of addition are clearly of the same order of magnitude, while the absolute calculated values are 3 kcal/mol too high.

The kinetically more favorable orientation of insertion (1,2) is calculated to give a product that is thermodynamically less favorable. The thermodynamic difference between the 2,1- and 1,2-insertion products is calculated to be 4.9 kcal/mol for the ^{Me}PCP species and 16.5 kcal/mol for the ^{tBu}PCP complex. This suggests that steric effects play a dominant role in favoring the thermodynamics of the product with the phenyl group bound to the *β*-carbon, while also playing a dominant role in *disfavoring* the kinetics of formation of the same complex, as discussed above.

In particular, it should be noted that the 1,2-insertion is 19.8 kcal/mol exoergonic for the ^{Me}PCP complex at 25 °C (see Figure 16); that is, it is calculated to be effectively irreversible. In contrast, the calculations predict that the free energy of 1,2-insertion into the Ir−H bond of the ^{tBu}PCP complex (**3′**, to give **4a′**) is −3.2 kcal/mol, and therefore effectively *reversible*. This result is in excellent agreement with the observation of reversible insertion (eq 10) and, quantitatively, with the experimental free energy value of −3.8 kcal/mol (25 °C) for insertion to give **4a**.

Thus the calculated energies strongly indicate that the highly unusual *β*-vinyl-hydrogen elimination from **4** (eq 10) is thermodynamically possible because of the unusual degree of crowding. Considering the presence of the bulky *t*-butyl groups on phosphorus and the sterically demanding phenyl group at the α position it seems reasonable that complex **4a** might be unusually unfavorable thermodynamically. Inspection of the calculated structure of **4a′** indeed reveals significant crowding, and the contrast with the less crowded 2,1-insertion product **6′** is evident (Figure 17).

In both structures **4a′** and **6′**, the PCP ligand is "twisted" such that the *t*-butyl groups immediately above and below the vinyl group maximize their distance from that group. In the case of **4a′**, however, numerous short interatomic distances between the phenyl group and the PCP and acetylide ligands are present in spite of this twisting (Figure 17). Furthermore, the greater twisting of the PCP group in **4a′** versus **6′** results in short contacts between those *t*-butyl groups that are on the side opposite the phenylvinyl group (including the H−H distance of 1.93 Å indicated in Figure 17).

8b. C−C elimination. The most surprising conclusion of our experimental studies is that C−C bond elimination from acetylide−vinyl species is disfavored by the presence of either electron-donating or -withdrawing substituents on the α-carbon of the vinyl group. Thus, increased steric bulk apparently *disfavors* elimination. This counterintuitive conclusion is well supported by calculations. The barrier to elimination from the α-phenylvinyl complex **4a′** is calculated to be 25.8 kcal/mol. Although the less crowded *β*-phenylvinyl complex **6′** is thermodynamically much more stable (by 16.5 kcal/mol), it has a much lower calculated barrier to C−C elimination, just 17.9 kcal/mol, and the TS is 1.8 kcal/mol below reactants in free energy (Figure 15). Also in accord with C−C elimination being inhibited by crowding, the calculated values for the barrier to elimination are substantially lower for the less crowded ^{Me}PCP analogues: 17.3 kcal/mol for **4″** and 12.4 kcal/mol for **6″**.

Thus, the α-phenyl species (**4′** and **4″**) are higher in energy than the *β*-phenyl isomers, as expected on the basis of steric considerations but, unexpectedly, they also have higher barriers to elimination. Together these two factors result in very large differences for the total TS free energies of elimination: 24.4 kcal/mol for the ^{tBu}PCP complexes (22.6 kcal/mol (**TS-4a′-elim**) − (−1.8) kcal/mol (**TS-6′-elim**), Figure 15). This overall difference strongly supports the idea that the observed regioselectivity may be viewed as being controlled by the kinetics of C−C elimination. For the ^{Me}PCP complexes, the difference is considerably smaller, 9.8 kcal/mol, in support of the conclusion that the difference in activation energies reflects steric effects.

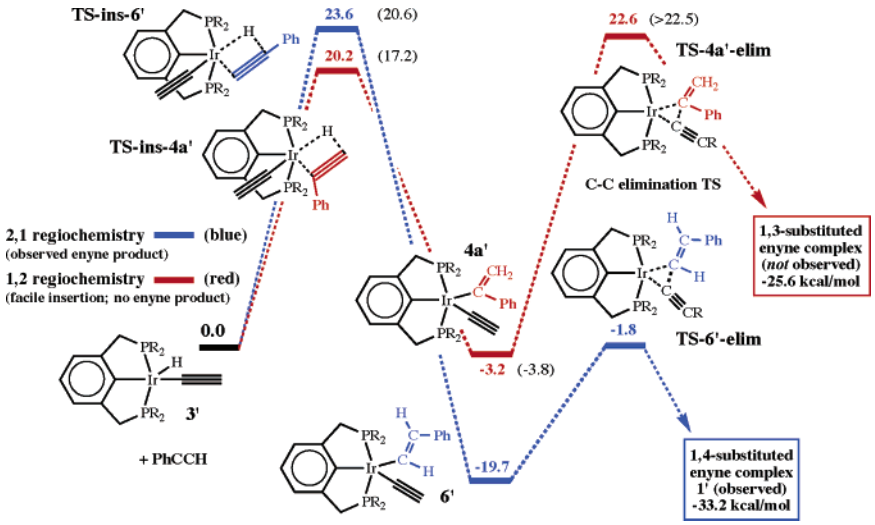

Figure 15. Calculated free energy profile (25 °C) for the reaction of ($^{t\text{Bu}}$PCP)Ir(H)(CCH) with phenylacetylene. The experimentally observed 2,1-regiochemistry is in blue and the 1,2-regiochemistry (not observed) is in red. Experimental values (extrapolated to 25 °C) are shown in parentheses. The acetylide group (but not the incoming phenylacetylene) is truncated and modeled as a simple acetylide.

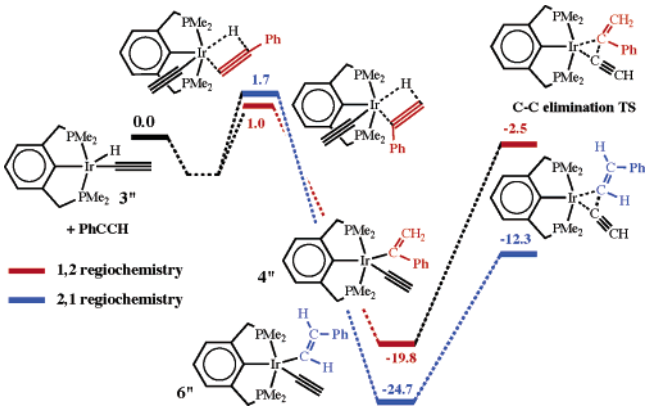

Figure 16. Calculated free energies for addition of the C−H bond of acetylene across the triple bond of phenyl acetylene with 2,1- and 1,2-regiochemistry for a model $^{\text{Me}}$PCP ligand. The acetylide group (but not the incoming phenylacetylene) is truncated and modeled as a simple acetylide.

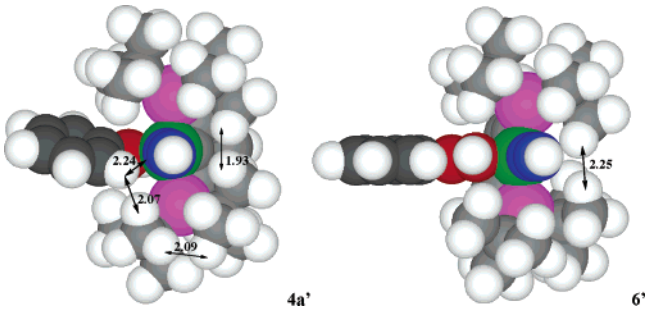

Figure 17. Calculated structures (atoms shown at 75% van der Waals radii) for ($^{t\text{Bu}}$PCP)Ir(acetylide)(phenylvinyl) isomers **4a′** (α-phenylvinyl) and **6′** (β-phenylvinyl). The perspective is approximately as viewed down the acetylide C−C axis, and atoms are shown at 75% van der Waals radii. Particularly short interatomic distances (Å) are indicated. Complex **4a′** is calculated to be 16.5 kcal/mol above **6′** in free energy.

The DFT calculations help to elucidate a very simple and compelling explanation for the slower elimination rates from the α-substituted vinyl complexes. The vinyl groups of all ($^{t\text{Bu}}$PCP)Ir vinyl complexes discussed in this work are approximately located in the plane bisecting the ($^{t\text{Bu}}$PCP)Ir moiety (or the plane bisecting the P−Ir−P axis.) This can be seen in the X-ray structure of complexes **5** and **7a**, as well as the CO

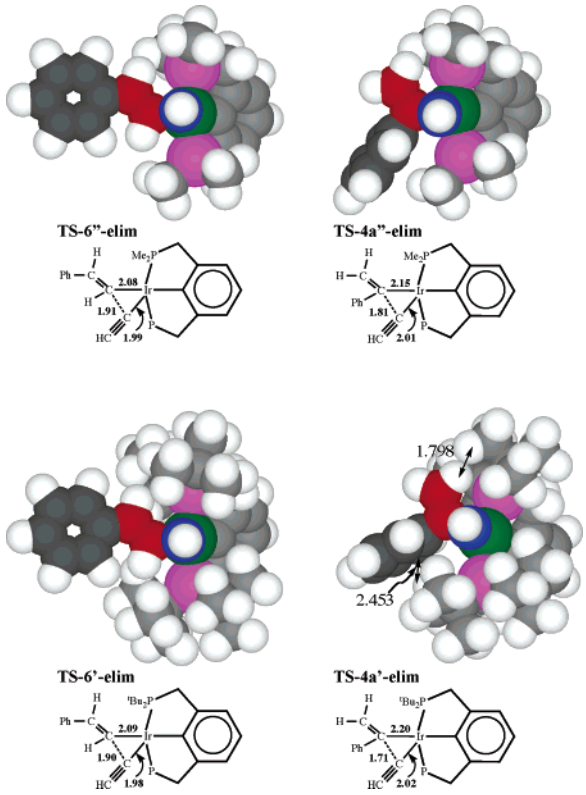

Figure 18. Calculated transition states (atoms shown at 75% van der Waals radii) for acetylide/phenylvinyl C−C elimination from ($^{\text{R}}$PCP)Ir(CCH)(*trans*-CH=CHPh) and ($^{\text{R}}$PCP)Ir(CCH)(CPh=CH$_2$) ($^{\text{R}}$PCP = $^{\text{Me}}$PCP and $^{t\text{Bu}}$PCP). The perspective is approximately as viewed down the acetylide C−C axis. Schematic structures shown with Ir−C and C−C distances (Å).

adducts **4-CO**, **5-CO**, **6-CO**, and **8-CO**. The calculated structures of **4a′** and **6′** (Figure 17) also reveal this structural motif.

In all the calculated TSs for C−C bond elimination (**TS**-X-elim), the vinyl groups are rotated approximately *perpendicular* to the plane bisecting the P−Ir−P axis, in contrast to the structures of the energy minima. This rotation presumably allows the use of the vinyl group π-system for incipient C−C bond formation. Figure 18 shows the structures of the calculated TSs, approximately as viewed down the acetylide C−C axis. Clearly, rotation of the vinyl group engenders substantial steric repulsion,

Scheme 3

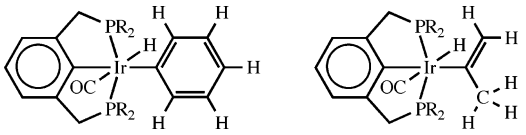

particularly in the α-phenylvinyl species and particularly with the $^{t\text{Bu}}$PCP ligand. For example, a vinyl-H/*t*-butyl-H distance of 1.80 Å and a phenyl-C/*t*-butyl-H distance of 2.45 Å are calculated for **TS-4a′-elim** (typical values for van der Waals radii of H and C are 1.2 and 1.7 Å, respectively[55]); no such close contacts are calculated for **TS-6′-elim**.

Although the vinyl acetylide C−C eliminations ultimately result in C−C σ-bond formation with no formal change in the vinyl π-bond, the C−C bond formation in the TS apparently uses the vinyl group π-system. To our knowledge this is not a well precedented model for C−C elimination. In the most comprehensive theoretical study of the reductive elimination of unsaturated hydrocarbyl groups to date, Musaev and Morokuma invoke the lesser directionality of sp^2 versus sp^3 carbon orbitals to explain the greater facility of vinyl versus methyl elimination (from Pd(II) and Pt(II)).[56] Our results indicate that the presence of a π-system in vinyl ligands, and perhaps the greater directionality of the carbon p-orbitals, is a major factor in the present system. Efforts to develop a detailed MO-based model for the involvement of π-systems in this and other C−C elimination reactions are currently underway.

We are aware of one example of C−C elimination in which the ligand π-system appears to play a key role: Morokuma and co-workers,[57] in modeling C−C reductive elimination from ruthenium in the Murai system, proposed an attack by an alkyl group on an aryl group. In that case, the aryl group is constrained by chelation to face the attacking alkyl group. In the present system, steric effects significantly hinder the ability of the vinyl group to rotate so as to face the acetylide group. The energetic cost is prohibitive, when the vinyl group has an α-substituent, and the feasibility of vinyl-group rotation ultimately appears to determine the directionality of the overall dimerization reaction.

9. An Experimentally Determined Barrier to Rotation. A key conclusion from the above computational studies is that the phosphinoalkyl groups impose a significant barrier to a ca. 90° rotation around the Ir−C(vinyl) bond, which in turn substantially increases the barrier to C−C bond elimination. As a means to determine the magnitude of such barriers to rotation we considered dynamic NMR studies of the complex ($^{t\text{Bu}}$PCP)-Ir(CO)PhH, in which rotation around the Ir−C(phenyl) bond is a degenerate event. (Note that the five-coordinate species ($^{t\text{Bu}}$-PCP)IrPhH undergoes facile elimination of benzene, which precludes its use for this purpose.) In steric terms, the phenyl group is probably about equivalent to an α-methylvinyl group (and probably not very different from an α-phenylvinyl group), as indicated in Scheme 3.

In the low-temperature limit (ca. ambient temperature or below) the ortho protons of the ($^{t\text{Bu}}$PCP)Ir(CO)PhH phenyl group appear as two signals, each one a doublet split by the respective neighboring meta-proton (the signal due to one of the meta-protons overlaps with that of C_6D_5H and was not used for fitting). Warming the sample results in line broadening, reaching coalescence at about 60 °C. With the use of the program WinDNMR,[58] the spectra can be modeled nearly perfectly over the range 25−75 °C, assuming exchange between the two protons, which presumably results from rotation about the Ir−C bond. An Eyring plot of ln(*k*/*T*) versus 1/*T* gives a straight line ($R^2 = 0.995$) with slope and intercept of −8343 deg and 23.136, respectively, which yields $\Delta H^{\ddagger} = 16.6$ kcal/mol and $\Delta S^{\ddagger} = -1.2$ eu. The activation free energy barrier to rotation is thus $\Delta G^{\ddagger} \approx 17$ kcal/mol. Such an energetic contribution (or even a substantial fraction thereof) to the barrier to C−C elimination would reduce the overall reaction rate by many orders of magnitude.

Conclusions

A combined experimental/computational study of arylacetylene dimerization promoted by (PCP)Ir has revealed fundamental and surprising aspects of (i) the addition of metal-hydrogen bonds across C−C triple bonds and, in particular, (ii) carbon−carbon reductive elimination.

(i) Insertion of the triple bond of phenylacetylene into the Ir−H bond of ($^{t\text{Bu}}$PCP)Ir(CCPh)H proceeds readily, and reversibly, even at −35 °C. To our knowledge, this is the first example of reversible addition of a metal-hydride bond across a C−C triple bond and, indeed, the first example of β-H elimination from a metal−vinyl complex to give a nonbridging metal hydride. This unusual behavior is attributable in large part to crowding in the vinyl acetylide complex, which favors the thermodynamics of acetylene deinsertion.

The facile insertion proceeds with the wrong orientation (1,2) to afford the observed enyne product; the reversibility is therefore key to the enyne formation, in that the alkyne ultimately undergoes an insertion with the "correct" (2,1) orientation.

(ii) The failure of the 1,2-insertion product (i.e., the iridium(α-phenylvinyl)(acetylide) complex, **4**) to undergo C−C elimination to give enyne is attributable to steric effects exerted by the phenyl group at the α position. In support of this conclusion vinyl−acetylide elimination also fails to occur for analogous α-methylvinyl (**7**) and α-vinylvinyl (**8**) acetylide complexes. The 2,1-insertion product (i.e., the iridium(β-phenylvinyl)-(acetylide) complex, **6**) does undergo elimination to give the observed product; this is confirmed by independent synthesis of **6**. Thus, even though elimination alleviates crowding, there is a *greater* barrier for elimination of the sterically *more* hindered vinyl groups.

DFT calculations allow the elucidation of a clear explanation for the inhibition of elimination owing to the α-vinyl substituents. In the energy minima, the vinyl groups rest approximately in the plane perpendicular to the P−P axis. In the elimination TS's however, the vinyl groups are rotated by 90° to allow an attack of the acetylide group on the vinyl π-system. This rotation is substantially inhibited by the presence of α-vinyl substituents.

We believe that the observation of steric inhibition of C−C bond elimination, and the conclusion that vinyl groups must orient in a specific direction to undergo C−C bond formation,

(55) Bondi, A. *J. Phys. Chem.* **1964**, *68*, 441−451.
(56) Ananikov, V. P.; Musaev, D. G.; Morokuma, K. *Organometallics* **2005**, *24*, 715−723.
(57) (a) Matsubara, T.; Koga, N.; Musaev, D. G.; Morokuma, K. *J. Am. Chem. Soc.* **1998**, *120*, 12692−12693. (b) Matsubara, T.; Koga, N.; Musaev, D. G.; Morokuma, K. *Organometallics* **2000**, *19*, 2318−2329.
(58) Reich, H. J. *J. Chem. Educ.: Software, Ser. D* **1996**, *3D*, 17−19.; 27−33.; 56−66.

may have significant implications for the understanding and design of other C−C bond formation systems.

General Experimental Methods and Computational Details

General Experimental Methods. All reactions, recrystallizations, and routine manipulations were performed at ambient temperature in an argon-filled glove box, or under argon using standard Schlenk techniques. Benzene and *p*-xylene were distilled from sodium/potassium alloy and vacuum transferred under argon. Deuterated solvents for use in NMR experiments were dried as their protiated analogues. (PCP)-IrH_2 was synthesized according to published methods.[59] All other chemicals were used as received from commercial suppliers. ^1H and $^{31}P\{^1H\}$ NMR spectra were obtained on a 400-MHz, Varian Inova-400 spectrometer or on a 300-MHz, Varian Mercury-300 spectrometer. ^1H chemical shifts are reported in ppm downfield from tetramethylsilane and were referenced to residual protiated (^1H) or deuterated solvent. ^{31}P NMR chemical shifts were referenced to 85% H_3PO_4. Mesitylene was employed as an internal standard when yields were determined by NMR spectroscopy. (*E*)-1,4 diphenyl-1-buten-3-yne was independently synthesized by a literature procedure.[60] Experimental details and spectroscopic characterizations are present in the Supporting Information.

Computational Details. The electronic structure calculations employed the DFT method[61] with the PBE[53] exchange and correlation functionals. The relativistic, small-core ECP and corresponding basis sets (6s5p3d) of Dolg et al. were used for the Ir atom (SDD model).[62] We used all-electron, full double-ζ plus polarization function D95(d) basis sets[63] for the C atoms in the acetylene adducts. Carbon atoms in the PCP unit were also covered with the D95(d) basis set in calculations where the representation of the PCP species was truncated and placed methyl groups on the P atoms (i.e., $PR_2 = PMe_2$). Most calculations were made modeling the PCP species with the *t*-Bu groups actually used in the experiments, $PR_2 = P(t\text{-Bu})_2$. The C atoms (and their attached H atoms) in the *t*-Bu groups were then described by the minimal STO-3G basis set.[64] Regular hydrogen atoms carried a double-ζ quality 21G basis set,[65] whereas acetylenic hydrogen atoms, which formally become hydrides in the metal complexes, were described by the triple-ζ plus polarization 311G(p) basis set.[66]

Reactant, transition state, and product geometries were fully optimized, and the stationary points were characterized further by normal-mode analysis. The (unscaled) vibrational frequencies formed the basis for the calculation of vibrational zero-point energy (ZPE) corrections. Standard thermodynamic corrections (based on the harmonic oscillator/rigid rotor approximations and ideal gas behavior) were made to convert from purely electronic reaction or activation energies (ΔE, $\Delta E^{\ddagger}$; no ΔZPE) to (standard) enthalpies (ΔH, $\Delta H^{\ddagger}$; ΔZPE included) and free energies (ΔG, $\Delta G^{\ddagger}$; $T = 298$ K, $P = 1$ atm).[67] All calculations were executed using the Gaussian 03 series of computer programs.[68]

We also carried out a large number of calculations on the acetylene dimerization reaction profile with a variety of two-layer ONIOM-type approaches (DFT/MM; DFT/HF; DFT/DFT) in which the four *t*-Bu groups were treated as the "low level" layer.[69] The results of these calculations will not be discussed in detail here, but we did make some comparisons to the experimental kinetic and thermodynamic observations described above and found that the ONIOM-type approaches consistently overestimated the steric repulsions exerted by the *t*-Bu groups. In particular, the largest disagreements with the experimental data were shown by the computationally most efficient ONIOM approach in which the *t*-Bu groups were represented using a molecular mechanics force field (UFF).[70] As the sophistication in the treatment of the "low level" layer increased, for example from replacing the UFF treatment by a small basis set ab initio Hartree−Fock or DFT treatment, the strong overestimation of steric effects attenuates slowly. As the computational treatment of the *t*-Bu groups approaches the high level applied to the remainder of the (PCP)Ir-acetylene species, the agreement between computed and experimentally derived data gradually improves; regular all-electron DFT-type calculations on the entire molecular species clearly provide the best description of the chemistry observed here. We have actually computed most species with both B3LYP[54] and PBE functionals, but results presented in the discussion, unless noted otherwise, were obtained using the PBE functionals which uniformly gave results in much better agreement with experiment.

Acknowledgment. Financial support by the National Science Foundation (Grant CHE-0316575, and Grant CHE-0091872 for purchase of the Bruker SMART APEX diffractometer) is gratefully acknowledged.

Supporting Information Available: Crystallographic data for complexes **1**, **3**, **4-CO**, **5-CO**, **5**, **6-Ar-CO**, **7a**, **8-CO**, and (PCP)Ir(CO) cocrystallized with **2**; experimental details and spectroscopic characterization of all complexes; complete ref 68. This material is available free of charge via the Internet at http://pubs.acs.org.

JA0647194

(59) (a) Gupta, M.; Hagen, C.; Flesher, R. J.; Kaska, W. C.; Jensen, C. M. *Chem. Commun.* **1996**, 2083−2084. (b) Zhu, K.; Achord, P. D.; Zhang, X.; Krogh-Jespersen, K.; Goldman, A. S. *J. Am. Chem. Soc.* **2004**, *126*, 13044−13053. (c) Goldman, A. S.; Ghosh, R. In *Handbook of C-H Transformations - Applications in Organic Synthesis*; Dyker, G., Ed.; Wiley-VCH: New York, 2005; pp 616−621.
(60) Moskalev, N. V.; Timoshchenko, L. V.; Filimonov, V. D. *Zh. Org. Khim.* **1991**, *27*, 2233.
(61) Parr, R. G.; Yang, W. *Density-Functional Theory of Atoms and Molecules*; University Press: Oxford, 1989.
(62) Dolg, M.; Wedig, U.; Stoll, H.; Preuss, H. *J. Chem. Phys.* **1987**, *86*, 866.
(63) Dunning, T. H.; Hay, P. J. Modern Theoretical Chemistry. In *Modern Theoretical Chemistry*; Schaefer, H. F., III, Ed.; Plenum: New York, 1976; pp 1−28.
(64) Hehre, W. J.; Stewart, R. F.; Pople, J. A. *J. Chem. Phys.* **1969**, *51*, 2657.
(65) Binkley, J. S.; Pople, J. A.; Hehre, W. J. *J. Am. Chem. Soc.* **1980**, *102*, 939.
(66) Krishnan, R.; Binkley, J. S.; Seeger, R.; Pople, J. A. *J. Chem. Phys.* **1980**, *72*, 650.
(67) McQuarrie, D. A. *Statistical Thermodynamics*; Harper and Row: New York, 1973.
(68) Frisch, M. J.; et al. *Gaussian 03*, revision B.02; Gaussian, Inc.: Wallingford, CT, 2004.
(69) Wüllen, C. J. v. *J. Comput. Chem.* **1997**, *18*, 1985−1992.
(70) Rappe, A. K.; Casewit, C. J.; Colwell, K. S.; Goddard, W. A., III; Skiff, W. M. *J. Am. Chem. Soc.* **1992**, *114*, 10024−10035.